Journal of Physics: Conference Series **565** (2014) 012011 doi:10.1088/1742-6596/565/1/012011

3D Mapping of plasma effective areas via detection of cancer cell damage induced by atmospheric pressure plasma jets

Xu Han[1,2], Yueing Liu[3], M. Sharon Stack[3,4] and Sylwia Ptasinska[1,2,3]*

[1]Radiation Laboratory, [2]Department of Physics, [3]Harper Cancer Research Institute, [4]Department of Chemistry and Biochemistry, University of Notre Dame, Notre Dame, IN, 46556, USA

E-mail: Sylwia.Ptasinska.1@nd.edu

Abstract. In the present study, a nitrogen atmospheric pressure plasma jet (APPJ) was used for irradiation of oral cancer cells. Since cancer cells are very susceptible to plasma treatment, they can be used as a tool for detection of APPJ-effective areas, which extended much further than the visible part of the APPJ. An immunofluorescence assay was used for DNA damage identification, visualization and quantification. Thus, the effective damage area and damage level were determined and plotted as 3D images.

1. Introduction

Atmospheric pressure plasma jets (APPJs) offer many opportunities for applications at the intersection of plasma physics, radiation chemistry and medicine [1]. Currently, much scientific effort is focused on ascertaining the effects of atmospheric pressure plasmas interacting with cancer cells (oral [2], prostate [3], skin [4], brain [5], pancreatic [6,7], melanoma [8], human breast [9], lung [10], and liver [11]), understanding the fundamental mechanisms that lead to cell death, and finding the optimal conditions for cancer treatment. These studies aim to explore the pros and cons of plasma radiation as an alternative to antitumor therapy. Our long-term goal is to elucidate whether the APPJ, which produces a cocktail of plasma species upon reactions with air and liquid, including charged particles (ions and electrons), photons, radicals and neutral species (excited atoms and molecules) can be controlled and targeted to selectively destroy cancer cells while causing little damage to the healthy tissue.

Our previous studies on damage induced to isolated DNA extracted from *E. coli* bacteria indicated that DNA is very sensitive to short-term APPJ exposure [12]. Extremely rapid degradation of DNA was observed, yielding 60% damage within the first 10 s of APPJ treatment [12]. We also observed that the influence of the medium (e.g., water [13,14] or amino acid solution [13]) has some effect on the level of DNA damage, but high percentages of DNA damage were still reached under these experimental conditions. Our studies on isolated DNA showed mainly the formation of single strand breaks, which can easily be repaired by the cell, as opposed to double strand breaks within the DNA molecule. Therefore, the question arose as to whether APPJ can induce damage to DNA in the cell, which is a much more complex biological system than the above mentioned media. The answer to this question would provide more insight into the possibility of using APPJ as a tool for cancer treatment.

* To whom any correspondence should be addressed.

Therefore, we recently performed a study to detect damage to DNA in cancer cells [2]. We observed that even short irradiation times by APPJ (< 30 s) caused destruction of DNA in 60% of cells [2]. This indicates a relatively fast cascade of biochemical reactions leading to multiple strand breaks in DNA initiated by the reactive species from the APPJ. For longer irradiation times, the damage level increases, reaching nearly 80% after only 2 min of APPJ treatment. At such prolonged irradiation times, the effective area of the APPJ is much larger than the area in which the APPJ is in direct contact with a sample [2]. This finding can have significant consequences for applications of APPJs, where the plasma has to be used for the treatment of localized areas (e.g., tumors) of a specific size or shape.

In this work, we discuss effective areas measured for our APPJ source, compare them with other effective areas obtained from various APPJ sources, and suggest a way to plot these areas as a 3D map.

2. Experimental set-up

Recently, we successfully constructed and developed various APPJ sources, which we used for the treatment of different materials such as semiconductors (e.g., Si) [15] and bio-macromolecules (e.g., DNA) [14]. The APPJ source used in this study operates based on a dielectric barrier discharge and consists of a dielectric tube (inner diameter of 2 mm, outer diameter of 3 mm) with two thin copper electrodes alternately wrapped around it in a spiral configuration [2,16], with one electrode connected to a high voltage (HV) power supply and the other to the ground (Fig. 1). Nitrogen gas (99.99% from Airgas, USA) was flowed through the dielectric tube at a flow rate of 1.5 slm. The gas discharge was ignited inside the tube by a relatively low-frequency (28 kHz) AC sinusoidal input with a peak-to-peak voltage of 22.4 kV and peak-to-peak current of 59 mA measured by voltage (Tektronix TCP A300) and current (Tektronix P6015A) probes, respectively. Once a plasma jet was launched outside the source, it formed an almost cylindrical jet.

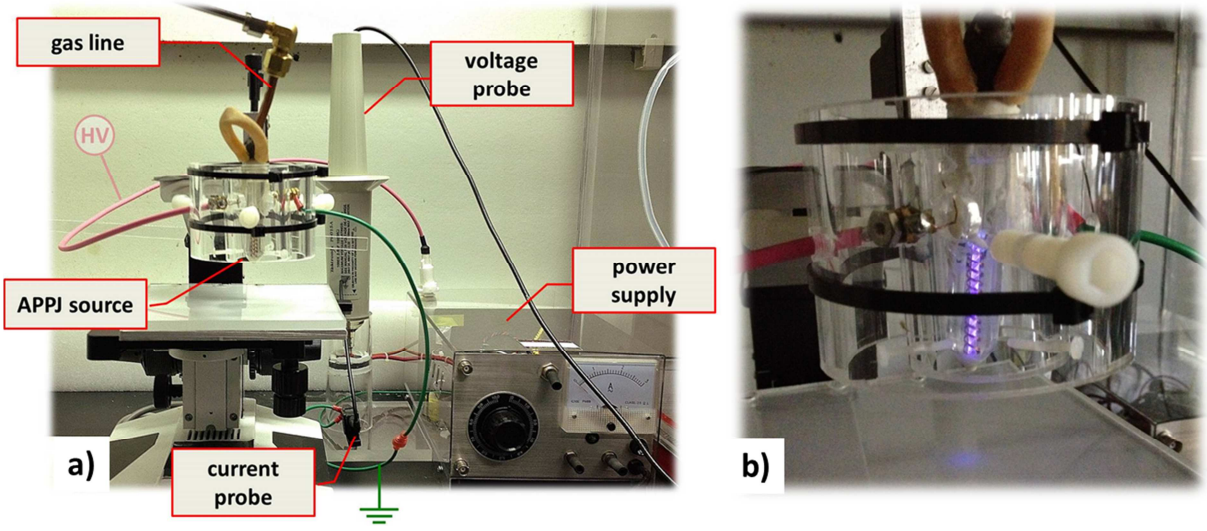

Figure 1. Experimental set-up of the nitrogen APPJ source used for treating cells (a) and the APPJ source in an operational mode (b).

Oral cancer cells (SCC-25) grown on photoetched coverslips were irradiated by the nitrogen APPJ to determine its effectiveness in inducing DNA damage [2]. Damaged DNA molecules served as surrogate markers for high-level damage in cells. To visualize damaged DNA in the nuclei, both treated and control cells were probed with H2AX antibody, followed by a fluorescently tagged secondary antibody (green fluorescence protein, GFP), and then imaged by fluorescence microscopy. Phosphorylated H2AX is a common marker used for DNA damage resulting from direct radiation and/or correlated to apoptosis. Therefore, in the present study, we are unable to determine the type of

DNA and cell alteration induced by APPJ treatment. By comparing the number of cells with GFP to the total number of nuclei stained by DAPI (4', 6-diamidino-2-phenylindole), the ratio of cells with DNA destroyed on the coverslip was obtained. This ratio of cells with DNA strand breaks over the total number of cells hereafter is called the damage ratio.

3. Results and discussion

Our previous studies showed that isolated DNA molecules that have been extracted from *E. coli* can be damaged by plasma radiation [12–14,17]. Damage levels in DNA were evaluated in terms of various distances from the source orifice and plasma exposure times. In the present study, we investigated damage to cellular DNA. It is worth noting that treatment with the plasma can affect cells on multiple levels, causing damage to cell walls (due to etching), the membrane (local disruption and lipid peroxidation), DNA (oxidative DNA damage, base modification, thymine dimer formations, and strand breaks), RNA (strand breaks) and proteins (oxidative protein damage, unfolding, and amino acid modifications) [18].

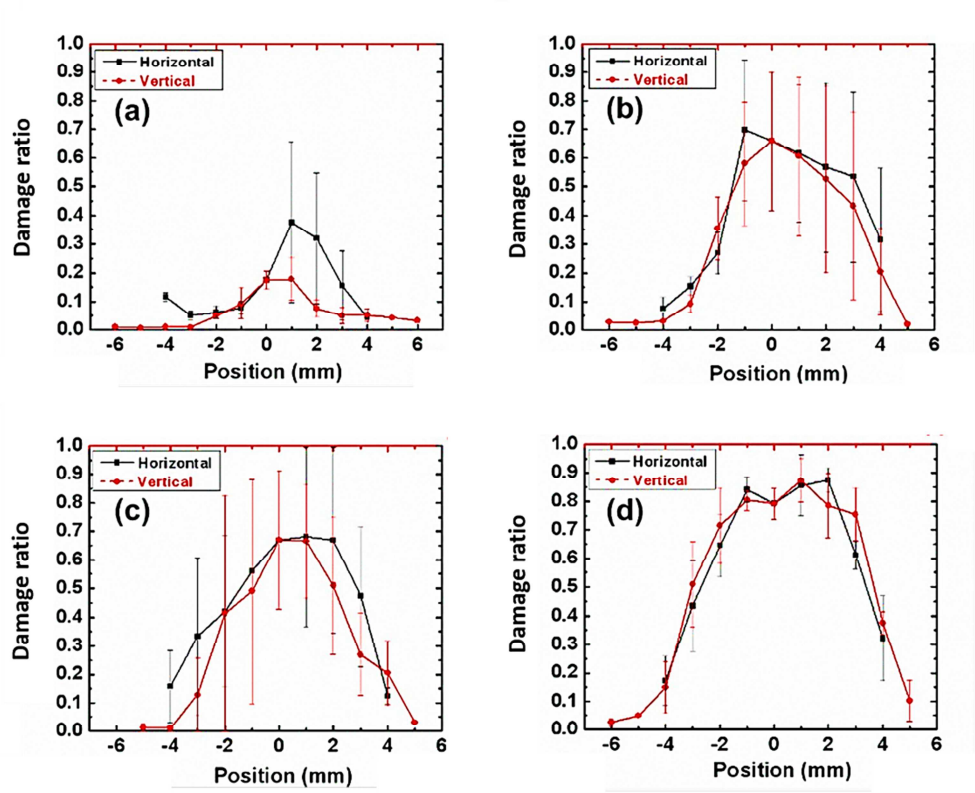

Figure 2. The damage ratio of cancer cells at different positions on the coverslip, which was placed at a distance of 2 cm from the source orifice, for various plasma treatment exposures: (a) 10 s, (b) 30 s, (c) 1 min and (d) 2 min. An error bar for each point was estimated as an average of two trials. Adapted from [2] with the permission of AIP Publishing LLC.

Since the diameter of our plasma jet was relatively small (~2 mm), we were interested in exploring how large an area can be affected by plasma irradiation. The obtained finding could provide significant information about the precision of plasma treatment when only a tumor area has to be targeted, while areas with healthy cells are intact. In this case, the ability to visualize damaged cells and distinguish them from intact cells is the key reason for choosing the technique of immunofluorescence microscopy for analysis of treated areas after plasma irradiation. In order to explore the effective area of plasma irradiation, the damage ratio was plotted in terms of spatial

parameters for four different plasma treatment durations. Figure 2 shows damage ratios at different positions on the coverslip detected in two perpendicular directions (labelled as "vertical" and "horizontal") from the point of direct APPJ contact with the sample. The damaged cell ratio was observed to increase with plasma irradiation time, reaching 40% after 10 s and 90% after 2 min. Moreover, the increase of plasma treatment time contributed to an enlargement in spatial peak widths, indicating larger effective areas for the APPJ. After a treatment of 10 s, the width of the plotted peaks corresponded to that of the diameter of the visible part of APPJ; however, after 2 min treatment, the width was five times larger than the diameter of the APPJ.

In order to obtain detailed information on the effective area of the APPJ, a 3D map was plotted for two coverslips with cancer cells treated by APPJ radiation over 10 s and 2 min (Fig. 3). The data in Figure 3 represent one set of multiple experimental trials performed under the same conditions as those in Figure 2. The damage level increased significantly with APPJ exposure time as is shown also in Figure 2, as did the area in which damaged cells were detected. For these two particular trials, the damage ratios in Figures 3a and 3b were estimated to be 20% and 66%, respectively. The estimated effective area from Figure 3b was ~ 50 mm^2, while the area of direct contact of the visible part of the APPJ with the sample was ~5 mm^2. Since the diameter of the plasma jet is very small, the damaging effects acting on locations distant from the center are not likely to be due to direct interactions of the APPJ with the cells. Rather, these damaging effects are likely due to secondary interactions as a result of the diffusion of reactive radical species and electrons generated in the APPJ, followed by complex chemical reactions activating cells to cause DNA strand breaks. This assumption is also supported by the work of the Laroussi group [19] and other groups discussed below, who found a similar effect of plasma acting on bacteria; in their studies, a larger inactivation area of bacteria was observed with a longer plasma treatment.

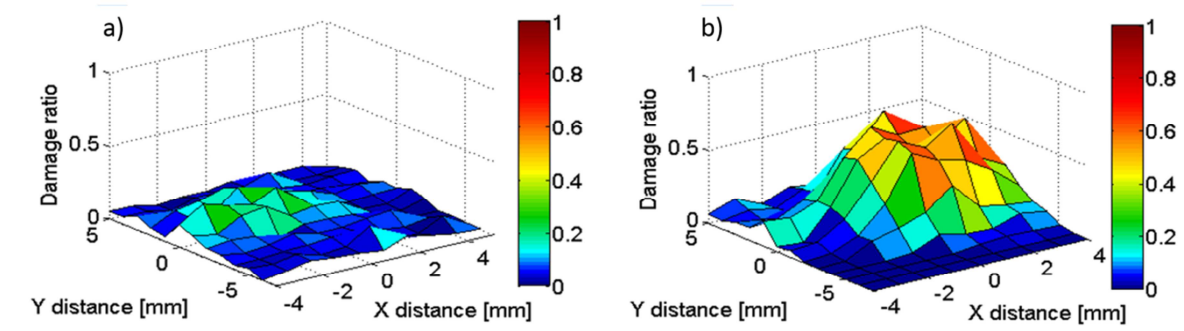

Figure 3. Spatial distributions of damage ratio of cancer cells placed at a distance of 2 cm from the source orifice and irradiated by the APPJ for 30 s (a) and 120 s (b).

Additionally, in our recent study, we investigated the extent of the APPJ effective area by exposing samples of dry plasmid DNA to APPJ [17]. The radial and axial lengths of the visible part of the APPJ were 4 mm and 55 mm, respectively; however, DNA damage was detected at distances of 20 mm radially and 250 mm axially from the plasma source orifice. We found that the volume of the physical extent of the APPJ is about 50 times greater than that of the visible part. While the chemical composition of the visible part of the APPJ was identified by an optical emission spectroscopy, the detection of reactive species beyond this part could not be measured due to their significantly lower emission signals. Nevertheless, we proposed that the DNA damage at long distances is caused by reactive oxygen species [17].

As mentioned above, other groups have also observed enlarged effective areas of APPJs in comparison with the visible jet diameter. Most such investigations were performed with an APPJ used for bacterial inactivation [19–22]. In a study conducted by Deng et al. [20], the diameter of the

dielectric tube was about 6 mm; thus, the area of plasma treatment was estimated to be < 1 cm^2. However, the effective area of inactivation was much larger, particularly for longer APPJ exposure (~5 min). The diameters of the inhibition region were 1 and 3.5 cm after 0.5 and 5 min treatments, respectively. These authors suggested that the diffusion of reactive plasma species and also the presence of UV photons were the main factors for an enlarged sterilized zone.

Another group reported studies of atmospheric pressure plasma effects on different types of bacteria (*B. cereus*, *S. aureus*, *E. coli* and *P. aeruginosa*), which suggest possible applications of plasmas for the decontamination of surfaces [21]. All the tested bacteria treated by plasma exhibited the presence of clear zones, where growth was inhibited. The measured diameters of these zones increased with treatment times between 30 s and 2 min, and in all cases were extended beyond the visible plasma part that was < 5 mm in diameter at the point of direct contact with the sample. Additionally, the effective area varied for different types of treated bacteria with *P. aeruginosa* being the least susceptible to inactivation by APPJ exposure [21].

Colagar et al. [22] also concluded that an increase in APPJ exposure time led to more efficient and larger areas of *E. coli* inactivation. They reported that the area of the inactivation zone was increased 1.3% at 1.5 min compared with 1 min of APPJ exposure, while the area of the inactivation zone after 5.5 min was approximately three times greater than the area of the inactivation zone after 1 min irradiation.

In contrast to our studies with cancer cells [2] and studies performed by other groups on bacterial cells [19–22], in which the effective plasma areas expanded with increasing exposure time, a study on cell permeabilization using an APPJ showed that the effective areas are limited to the area at which the plasma comes in direct contact with the sample [23]; however, only short exposure treatments (1-30 s) were used for this investigation [23].

Other techniques have also been used to investigate the effective size of APPJs, mainly water contact angle measurements before and after surface treatment [24]. The contact angle on a clean glass surface before the plasma treatment was between 40-50º. After exposure to the APPJ, the treated surface became more hydrophilic with the contact angle < 10º, and the width of the treated area was ~25 mm. In order to eliminate ambient air diffusion and entrainment, an additional dielectric tube was placed around the APPJ. In this case, the treated area showed a similar change in hydrophilicity, but the effective area width was ~60 mm. This observation clearly indicates the possibility of controlling the effective area of plasma treatment [24].

4. Conclusions

In the present study, cancer cells grown on coverslips and then irradiated by an APPJ have been used to detect cells with damaged DNA and to measure the spatial distribution of plasma effective areas. The trends of all measured distributions suggested a lower number of cells with damaged DNA located farther from the irradiation center, where the APPJ was in direct contact with the sample. A comparison of the peak widths indicated a direct correlation between plasma effective area and treatment time. Mapping of damaged cells can be used as a method for determining the extent of any kind of plasma jet; however, the mechanism underlying the observed spread in damage needs to be further investigated.

Moreover, these enhancements in our knowledge of the effective plasma area can contribute to the further development and improvement of plasma therapeutic techniques.

Acknowledgments

This material is based upon work supported by the U.S. Department of Energy Office of Science, Office of Basic Energy Sciences under Award Number DE-FC02-04ER15533. This is contribution number NDRL 5035 from the Notre Dame Radiation Laboratory.

References

[1] Von Woedtke T, Reuter S, Masur K and Weltmann K-D 2013 *Phys. Rep.* **530** 291–320

[2] Han X, Klas M, Liu Y, Stack M S and Ptasinska S 2013 *Appl. Phys. Lett.* **102** 233703
[3] Hirst A M, Frame F M, Maitland N J and O'Connell D 2014 *Biomed Res. Int.* **2014** 878319
[4] Kim P Y, Kim Y-S, Koo I G, Jung J C, Kim G J, Choi M Y, Yu Z and Collins G J 2011 *PLoS One* **6** e24104
[5] Tanaka H, Mizuno M, Ishikawa K, Nakamura K, Kajiyama H, Kano H, Kikkawa F and Hori M 2011 *Plasma Med.* **1** 265–77
[6] Partecke L I, Evert K, Haugk J, Doering F, Normann L, Diedrich S, Weiss F-U, Evert M, Huebner N O, Guenther C, Heidecke C D, Kramer A, Bussiahn R, Weltmann K-D, Pati O, Bender C and von Bernstorff W 2012 *BMC Cancer* **12** 473
[7] Brullé L, Vandamme M, Riès D, Martel E, Robert E, Lerondel S, Trichet V, Richard S, Pouvesle J-M and Le Pape A 2012 *PLoS One* **7** e52653
[8] Sensenig R, Kalghatgi S, Cerchar E, Fridman G, Shereshevsky A, Torabi B, Arjunan K P, Podolsky E, Fridman A, Friedman G, Azizkhan-Clifford J and Brooks A D 2011 *Ann. Biomed. Eng.* **39** 674–87
[9] Kim S J, Chung T H, Bae S H, Leem S H 2010 *Appl. Phys. Lett.* **97** 023702
[10] Kim J Y, Ballato J, Foy P, Hawkins T, Wei Y, Li J and Kim S-O 2011 *Biosens. Bioelectron.* **28** 333–8
[11] Zhang X, Li M, Zhou R, Feng K and Yang S 2008 *Appl. Phys. Lett.* **93** 021502
[12] Ptasińska S, Bahnev B, Stypczyńska A, Bowden M, Mason N J and Braithwaite N S J 2010 *Phys. Chem. Chem. Phys.* **12** 7779–81
[13] Stypczyńska A, Ptasińska S, Bahnev B, Bowden M, Braithwaite N S J and Mason N J 2010 *Chem. Phys. Lett.* **500** 313–7
[14] Han X, Cantrell W A, Escobar E E and Ptasinska S 2014 *Eur. Phys. J. D* **68** 46
[15] Zhang X and Ptasinska S 2014 *J. Phys. D. Appl. Phys.* **47** 145202
[16] Klas M and Ptasinska S 2013 *Plasma Sources Sci. Technol.* **22** 025013
[17] Bahnev B, Bowden M D, Stypczyńska A, Ptasińska S, Mason N J and Braithwaite N S J 2014 *Eur. Phys. J. D* **68** 140
[18] Lackmann J-W and Bandow J E 2014 *Appl. Microbiol. Biotechnol.* **98** 6205–13
[19] Laroussi M, Tendero C, Lu X, Alla S and Hynes W L 2006 *Plasma Process. Polym.* **3** 470–3
[20] Deng S, Cheng C, Ni G, Meng Y and Chen H 2008 *Jpn. J. Appl. Phys.* **47** 7009–12
[21] Alkawareek M Y, Algwari Q T, Gorman S P, Graham W G, O'Connell D and Gilmore B F 2012 *FEMS Immunol. Med. Microbiol.* **65** 381–4
[22] Colagar A H, Memariani H, Sohbatzadeh F and Omran A V 2013 *Appl. Biochem. Biotechnol.* **171** 1617–29
[23] Leduc M, Guay D, Leask R L and Coulombe S 2009 *New J. Phys.* **11** 115021
[24] Hsu C and Yang Y 2010 *IEEE Trans. Plasma Sci.* **38** 496–9